precession photographs of a red lathe-shaped crystal. Accurate unit cell dimensions, derived from a least-squares refinement of 22 reflections for which $14° < \theta < 17°$, λ(Mo K$\bar{\alpha}$) = 0.710 69 Å, are as follows: a = 10.428 (4) Å, b = 16.616 (4) Å c = 12.402 (4) Å, β = 111.13 (3)°, D_{exptl} = 1.37 g cm^{-3}, Z = 4, V = 2004.4 Å^3. The space group was determined to be Cc, based on Z and the lack of symmetry in the molecule. Data were collected on a Philips diffractometer equipped with a graphite monochromator, Mo K$\bar{\alpha}$ radiation, using the θ–2θ scan technique, with a scan width of (1 + 0.3 tan θ), a scan rate of 0.01°/s for $\theta < 18°$ and 0.007°/s for $\theta \geq 18°$, $2° < \theta < 27°$, and background time equal to half the scan time. Intensities of three standard reflections were monitored every 2 h. These showed no appreciable change during the data collection. Data were processed by using a locally written program. No absorption correction was considered to be necessary (μ = 7.0 cm^{-1}, crystal dimensions 0.038 × 0.075 × 0.38 mm). A total of 1974 unique reflections were processed, of which 1362 had $I > 3\sigma(I)$ and were used in subsequent calculations. The function minimized was $\sum w(|F_o| - |F_c|)^2$ with $w = 1/\sigma^2|F_o|$.[33] Atomic scattering factors for neutral Fe, P, O, and C were taken from a recent tabulation,[34] those for H were taken from Stewart et al.,[35] and anomalous dispersion terms for Fe and P were included.[34]

The positions of iron and phosphorus atoms were determined from a Patterson map. All other non-hydrogen atoms were located on subsequent Fourier and difference Fourier maps. The two phenyl groups were treated as rigid hexagons, C–C = 1.395 and C–H = 1.0 Å. Hydrogen atoms of the methyl groups were placed in calculated positions (H–C–H = 109.5°, C–H = 1.0 Å) and were not refined. The remaining hydrogen atoms, which were all located in difference maps, were constrained to be 1.0 Å from their attached carbon atoms. Refinement of 149 parameters led to an agreement index of 0.0611 ($R = \sum||F_o| - |F_c||/\sum|F_o|$) and a weighted index of 0.0805 ($R_w = [\sum w(|F_o| - |F_c|)^2/\sum wF_o^2]^{1/2}$. A final difference electron density map showed no peaks greater than 0.5 e Å^{-3}.

Final positional parameters and their standard deviations are presented in Table II. Thermal parameters for non-hydrogen atoms, parameters for hydrogen atoms, and final values of observed and calculated structure factors are presented in Tables III, IV, and V, respectively, and are available as supplementary material.

Registry No. **5**, 66314-69-0; **8**, 90219-10-6; **9**, 90245-07-1; **10**, 90245-08-2; **12**, 90219-11-7; **13**, 90245-09-3; **14**, 90245-12-8; **15**, 90245-10-6; **16**, 90245-11-7; $Mn_2(CO)_{10}$, 10170-69-1; $[CpFe(CO)_2]_2$, 12154-95-9.

Supplementary Material Available: Tables of non-hydrogen atom thermal parameters (Table III), the hydrogen atom parameters (Table IV), and the structure factor amplitudes (Table V) (8 pages). Ordering information is given on any current masthead page.

(33) Sheldrick, G. M. "SHELX76", a Program for Crystal Structure Determination; University of Cambridge, England, 1976.
(34) "International Tables for X-Ray Crystallography"; Kynoch Press: Birmingham, England, 1974; Vol. IV.
(35) Stewart, R. F.; Davidson, E. R.; Simpson, W. T. *J. Chem. Phys.* **1965**, *42*, 3175.

A Theoretical Study of the Formation and Reactivity of Substituted Cyclohexadienyliron Complexes. The Structures and Reactivities of Tricarbonyl(2-methoxycyclohexadienyl)iron Cation and Tricarbonyl(1-methyl-4-methoxycyclohexadienyl)iron Cation

O. Eisenstein,*† William M. Butler,† and Anthony J. Pearson‡

Departments of Chemistry, The University of Michigan, Ann Arbor, Michigan 48109, and Case Western Reserve University, Cleveland, Ohio 44106

Received December 12, 1983

Extended Hückel calculations have been performed to understand the high regioselectivity in the formation and the reactivity of tricarbonyliron cyclohexadienyl cations. The formation of a substituted cyclohexadienyl complex from the diene complex by an hydride abstraction is rationalized. It is found that a distortion of the cyclohexadienyl complex in which the metal is not linked symmetrically to the two ends of the dienyl accounts for the high regioselectivity of the nucleophilic addition to the dienyl. This theoretical analysis is well supported by the structural determination of two cyclohexadienyl complexes: tricarbonyl(2-methoxycyclohexadienyl)iron cation and tricarbonyl(1-methyl-4-methoxycyclohexadienyl)iron cation.

Tricarbonyl(polyene)iron complexes are currently used in synthesis to allow an easy route to functionalized polyenes with special focus on cyclohexa-1,3-diene and cyclohexadienyl cation complexes. Converting one into the other presents some interesting and puzzling problems of regioselectivity.[1,2]

A tricarbonyl(cyclohexa-1,3-diene)iron complex, **1**, is easily converted into a cyclohexadienyl cation complex, **2**,

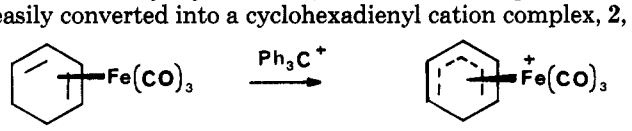

1 **2**

† University of Michigan. Present address of O.E.: Laboratoire de Chimie Theorique (CNRS, UA 506), Batiment 490, Centre de Paris-Sud, 91405 Orsay, France.
‡ Case Western Reserve University.

(1) Pearson, A. J. *Acc. Chem. Res.* **1980**, *13*, 463; *Transition Met. Chem. (Winheim, Ger.)* **1981**, *6*, 67 and references therein.

0276-7333/84/2303-1150$01.50/0 © 1984 American Chemical Society

by treatment with triphenylmethyl cation (trityl cation).[1] In an unsymmetrically substituted diene, **3**, the hydride abstraction is a regioselective reaction. If R is a π donor group such as OCH_3, the reaction produces 94% of isomer **4**, while if R is a π acceptor group such as CO_2CH_3, **5** is the major product (95%).[1] The reaction is evidently

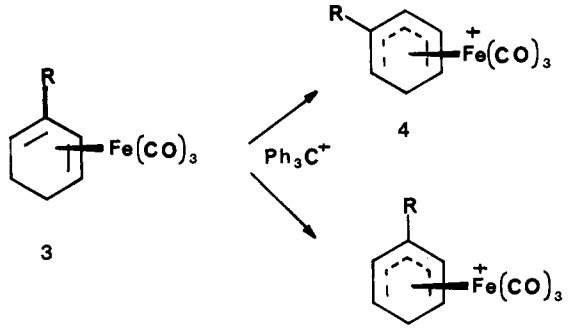

3 4 5

sensitive to steric factors. A 1-substituted diene complex gives predominantly a 1-substituted cyclohexadienyl complex. The case of a 1,4-disubstituted diene is more interesting because the steric factors may be equivalent for the two possible sites of abstraction. The treatment of **6** by the trityl cation provides **7**, in which the strongest π donor OMe occupies the same position as in **4**.

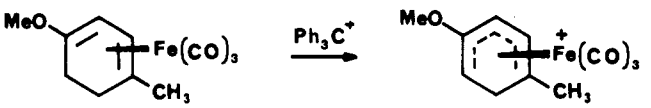

6 7

The reactivity of the cyclohexadienyl cation complex with nucleophiles has been widely studied.[1-4] It has been found that for a $Fe(CO)_3$ cyclohexadienyl complex, the addition of the nucleophile occurs exclusively at a terminal carbon to give a diene complex. An unsymmetrical substitution on the dienyl results in one of the terminal carbons being preferentially attacked. The 2-methoxycyclohexadienyl complex reacts at the C_5 position. Increasing the steric factors by a moderate degree at C_5 does not prevent the addition from occurring at the carbon in question. Thus in **8**, nucleophiles such as stabilized enolates add to C_5 to give **9**, although the ratio, addition to C_5 vs. addition to C_1, varies with the nature of the nucleophile and of the countercation.[3,4]

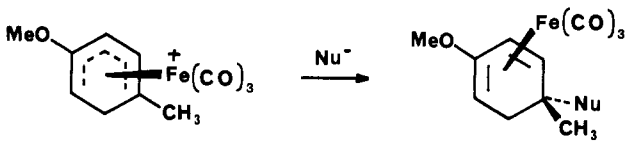

8 9

It has been proven by structural determination and kinetic studies that the nucleophile adds directly to the dienyl on the face opposite to that occupied by the metal.[5] It is believed that the reaction is kinetically controlled, although this is not certain with some nucleophiles.[6]

The reactivity of the tricarbonylcyclohexadienylosmium complex is somewhat different from that of an iron complex.[7] If the nucleophilic addition is not reversible (addition of H^- or CN^-), a σ–π-allyl complex, **10**, is formed. If the addition is reversible, the more stable 1,3-diene is obtained. σ–π-Allyl complexes are also obtained when tricarbonylcycloheptadienyl- and tricarbonylcyclooctadienyliron cation complexes react with nucleophile.[8] The relative stability of the σ–π-allyl and 1,3-diene complex for different ring sizes may orientate the reaction toward one of these products.

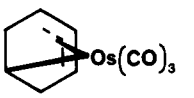

10

Despite the large body of experimental data, the chemistry of these molecules is not yet well understood. In addition, not many structures are known for the dienyl iron complexes because of crystallization problems. We are interested in exploring an eventual relation between the structure of unsymmetrical substituted cyclohexadienyl complexes and the observed high regioselectivity of their reactions.

In order to answer some of the above questions, we present here the results of a structural determination of tricarbonyl(2-methoxycyclohexadienyl)iron hexafluorophosphate salt (A) and of tricarbonyl(1-methyl-4-methoxycyclohexadienyl)iron hexafluorophosphate salt (B). A molecular orbital study based on extended Hückel calculations of the hydride abstraction from the diene complex and of the nucleophilic addition to the cyclohexadienyl cation complex is also presented. From the combination of structural and theoretical studies, it is possible to rationalize a large body of the experimental facts.

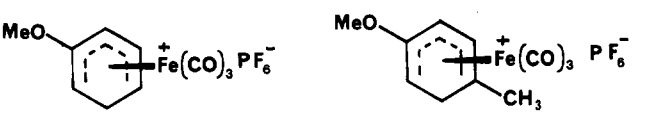

A B

Structure of the Two Cyclohexadienyliron Complexes: Salts A and B

Preparation. Complexes A and B were prepared by established literature procedures[9] and recrystallized as follows. Each was dissolved in the minimum volume of dichloromethane under nitrogen at room temperature. Ether was added to give a final

(2) Birch, A. J.; Bandara, B. M. R.; Chamberlain, K.; Chauncy, B.; Dahler, P.; Day, A. I.; Jenkins, I. D.; Kelly, L. F.; Khor, T.-C.; Kretschmer, G.; Liepa, A. J.; Narula, A. S.; Raverty, W. D.; Rizzardo, E.; Sell, C.; Stephenson, G. R.; Thompson, D. J.; Williamson, D. H. *Tetrahedron* **1981**, *37*, 289.

(3) Kelly, L.; Narula, A. S.; Birch, A. J. *Tetrahedron Lett.* **1979**, 4107; **1980**, 871. Birch, A. J.; Narula, A. S.; Dahler, P.; Stephenson, G. R.; Kelly, L. F. *Ibid.* **1980**, 979. Pearson, A. J.; Chandler, M. *J. Organomet. Chem.* **1980**, *202*, 175.

(4) Pearson, A. J.; Ham, P.; Ong, C. W.; Perrior, T. R.; Rees, D. C. *J. Chem. Soc., Perkin Trans. 1* **1982**, 1527. Pearson, A. J.; Perrior, T. R.; Rees, D. C. *J. Organomet. Chem.* **1982**, *226*, C39.

(5) Gower, M.; John, G. R.; Kane-Maguire, L. A. P.; Odiaka, T. I.; Salzer, A. *J. Chem. Soc., Dalton Trans.* **1979**, 2003. John, G. R.; Kane-Maguire, L. A. P. *Ibid.* **1979**, 873. Mansfield, C. A.; Kane-Maguire, L. A. P. *Ibid.* **1976**, 2187. Kane-Maguire, L. A. P.; Mansfield, C. A. *Ibid.* **1976**, 2192. Kane-Maguire, L. A. P. *J. Chem. Soc. A* **1971**, 1602. Birch, A. J.; Bogsanyi, D.; Kelly, L. F. *J. Organomet. Chem.* **1981**, *214*, C39.

(6) Birch, A. J.; Liepa, A. J.; Stephenson, G. R. *Tetrahedron Lett.* **1979**, 3565.

(7) John, G. R.; Kane-Maguire, L. A. P. *J. Chem. Soc., Dalton Trans.* **1979**, 1196. Deeming, A. J.; Ullah, S. S.; Domingos, A. J. P.; Johnson, B. F. G.; Lewis, J. *Ibid.* **1974**, 2093.

(8) Burrows, A. L.; Johnson, B. F. G.; Lewis, J.; Parker, D. G. *J. Organomet. Chem.* **1980**, *194*, C11. Edwards, R.; Howell, J. A. S.; Johnson, B. F. G.; Lewis, J. *J. Chem. Soc., Dalton Trans.* **1974**, 2105.

(9) Birch, A. J.; Chamberlain, K. B.; Haas, M. A.; Thompson, D. J. *J. Chem. Soc., Perkin Trans. 1* **1973**, 1882. Birch, A. J.; Cross, P. E.; Lewis, J.; Whike, D. A.; Wild, S. B. *J. Chem. Soc. A* **1968**, 332.

Table I. Summary of Data Collections and Processing Parameters for A and B

	A	B
space group	$P\bar{1}$	$P2_12_12_1$
a, Å	9.923 (3)	7.556 (2)
b, Å	7.059 (2)	13.556 (2)
c, Å	10.831 (3)	14.250 (3)
α, deg	108.82 (2)	90
β, deg	90.74 (2)	90
γ, deg	76.52 (2)	90
V, Å^3	696.8 (4)	1501.4 (5)
mol wt	393.99	408.02
Z	2	4
d(calcd), g/mL	1.88	1.81
cryst dimens	0.10 × 0.09 × 0.18	0.21 × 0.28 × 0.32
abs coeff, cm^{-1}	12.7	11.9
scan range, deg	Mo Kα − 0.8 to Mo Kα + 0.9	
bkgd time ratio	0.8	0.8
2θ, deg	45	50
data collected	1944	1699
data $>3\sigma$	1294	1357
final R_1	0.049	0.051
final R_2	0.056	0.069
parameters varied	199	208
quality-of-fit indicator	1.74	2.38
largest residual, e/Å^3	0.45	0.61
max shift/error	0.23	0.09

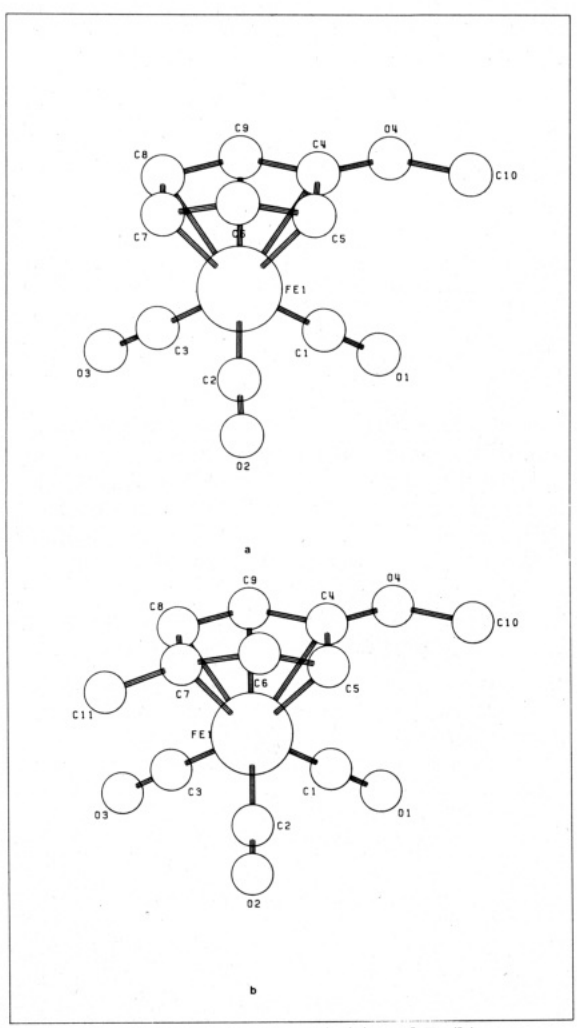

Figure 1. Molecular structure of A (a) and B (b).

mixture of approximately 80:20 CH_2Cl_2/Et_2O, and the solutions were set aside at −10 °C for several days, after which the crystals were removed by filtration in the usual way, washed with ether, and dried on a filter pad.

Table II. Positional Parameters for A and B[a]

atom	x	y	z
		a. A	
Fe1	0.1984 (1)	0.3054 (2)	0.1757 (1)
C1	0.2871 (8)	0.3733 (11)	0.0581 (8)
O1	0.3447 (7)	0.4192 (9)	−0.0131 (6)
C2	0.2859 (9)	0.0331 (13)	0.1138 (8)
O2	0.3445 (7)	−0.1329 (9)	0.0753 (6)
C3	0.0480 (9)	0.2879 (12)	0.0790 (8)
O3	−0.0465 (6)	0.2783 (10)	0.0214 (6)
C4	0.2705 (7)	0.5474 (10)	0.3247 (6)
O4	0.3342 (5)	0.6797 (7)	0.3011 (5)
C5	0.3384 (7)	0.3532 (11)	0.3325 (7)
C6	0.2656 (8)	0.2511 (12)	0.4035 (8)
C7	0.1238 (9)	0.2688 (13)	0.3537 (8)
C8	0.0528 (8)	0.4527 (15)	0.3401 (8)
C9	0.1242 (7)	0.5943 (10)	0.3221 (7)
C10	0.4832 (8)	0.6372 (13)	0.3008 (9)
P1	0.7628 (2)	0.0371 (3)	0.3041 (2)
F1	0.7920 (6)	−0.2028 (7)	0.2532 (7)
F2	0.8641 (5)	0.0280 (8)	0.4161 (5)
F3	0.6374 (6)	0.0518 (11)	0.3945 (6)
F4	0.6600 (6)	0.0442 (8)	0.1922 (5)
F5	0.7344 (7)	0.2746 (8)	0.3562 (7)
F6	0.8881 (7)	0.0175 (13)	0.2138 (7)
		b. B	
Fe1	0.6569 (2)	0.9335 (1)	1.0104 (1)
C1	0.7997 (14)	0.9184 (7)	1.1100 (6)
O1	0.8921 (11)	0.9082 (6)	1.1731 (5)
C2	0.4440 (15)	0.9558 (7)	1.0778 (6)
O2	0.3231 (11)	0.9705 (7)	1.1125 (5)
C3	0.6314 (13)	0.8050 (6)	0.9963 (7)
O3	0.6160 (13)	0.7256 (5)	0.9893 (6)
C4	0.8454 (12)	1.0424 (5)	0.9669 (5)
O4	1.0047 (8)	1.0581 (4)	1.0068 (4)
C5	0.6891 (10)	1.0866 (5)	0.9918 (6)
C6	0.5421 (12)	1.0934 (6)	0.9199 (6)
C7	0.5211 (12)	0.9921 (6)	0.8826 (6)
C8	0.6739 (12)	0.9419 (6)	0.8620 (5)
C9	0.8368 (12)	0.9633 (6)	0.9041 (5)
C10	1.0215 (15)	1.1348 (7)	1.0731 (7)
C11	0.3438 (15)	0.9628 (8)	0.8444 (7)
P1	1.0176 (4)	1.2448 (2)	0.7831 (2)
F1	1.1012 (19)	1.2429 (6)	0.6864 (6)
F2	0.9840 (10)	1.1333 (4)	0.7768 (4)
F3	0.8390 (17)	1.2637 (6)	0.7344 (10)
F4	1.1878 (11)	1.2281 (7)	0.8355 (10)
F5	0.9144 (13)	1.2523 (5)	0.8785 (6)
F6	0.9468 (13)	0.8573 (4)	0.7106 (4)

[a] Standard deviations for the last significant figures are given in parentheses.

X-ray Structures. Single crystals of A and B were mounted on a Syntex $P2_1$ diffractometer and the space groups determined. Table I contains a summary of data collection conditions and results. Lattice parameters were determined from a least-squares refinement of 15 reflection settings obtained from an automatic centering routine.

Intensity data were obtained by using Mo Kα radiation monochromatized from a graphite crystal whose diffraction vector was perpendicular to the diffraction vector of the sample. Three standard reflections were measured every 50 reflections. The data were reduced by procedures previously described.[10] Absorption correction was not necessary for either compound. The structures were solved by using MULTAN.[10] The function $\sum w(|F_o| - |F_c|)^2$ was minimized where $|F_o|$ and $|F_c|$ are the observed and calculated

(10) Computations were carried out on an Amdahl 470/V7 computer. Computer programs used during the structural analysis were SYNCOR (data reduction by W. Schmonsees), FORDAP (Fourier refinement by Z. Zalkin), ORFLS (full-matrix, least-squares refinement by Busing, Martin, and Levy), ORFFE (distances, angles, and their esd's by Busing, Martin, and Levy), ORTEP (thermal ellipsoid drawings by C. K. Johnson), HATOMS (hydrogen atom positions by A. Zalkin), PLANES (least-squares planes by D. M. Blow), ABSORB (Absorption correction program by D. Templeton and L. Templeton), and MULTAN78 by Petet Main.

Table III. Distances (Å) and Angles (deg) for A and B

a. A

Bond Distances

Fe1-C1	1.802 (10)	Fe1-C4	2.190 (7)	C4-C9	1.414 (9)	P1-F5	1.543 (5)
Fe1-C3	1.817 (8)	C1-O1	1.134 (9)	O4-C10	1.438 (9)	P1-F6	1.545 (6)
Fe1-C2	1.818 (9)	C2-O2	1.122 (8)	C5-C6	1.499 (10)	P1-F3	1.557 (6)
Fe1-C9	2.111 (7)	C3-O3	1.123 (8)	C6-C7	1.493 (11)	P1-F1	1.558 (5)
Fe1-C8	2.124 (7)	C4-O4	1.331 (8)	C7-C8	1.377 (11)	P1-F2	1.573 (5)
Fe1-C5	2.172 (6)	C4-C5	1.408 (9)	C8-C9	1.414 (11)	P1-F4	1.579 (5)
Fe1-C7	2.186 (8)						

Bond Angles

C1-Fe1-C3	92.31 (33)	C2-Fe1-C8	126.40 (37)	O1-C1-Fe1	178.04 (99)	F5-P1-F1	179.29 (64)
C1-Fe1-C2	94.66 (35)	C2-Fe1-C5	90.23 (30)	O2-C2-Fe1	177.34 (89)	F5-P1-F2	88.96 (31)
C1-Fe1-C9	102.01 (32)	C2-Fe1-C7	90.66 (34)	O3-C3-Fe1	178.66 (82)	F5-P1-F4	91.53 (31)
C1-Fe1-C8	138.87 (36)	C2-Fe1-C4	126.37 (29)	O4-C4-C5	124.76 (62)	F6-P1-F3	178.80 (56)
C1-Fe1-C5	99.95 (29)	C9-Fe1-C8	39.02 (30)	O4-C4-C9	116.40 (60)	F6-P1-F1	87.95 (41)
C1-Fe1-C7	165.05 (35)	C9-Fe1-C5	68.80 (25)	C5-C4-C9	118.13 (68)	F6-P1-F2	88.86 (36)
C1-Fe1-C4	86.11 (30)	C9-Fe1-C7	68.87 (30)	C4-O4-C10	118.52 (54)	F6-P1-F4	91.77 (37)
C3-Fe1-C2	96.77 (34)	C9-Fe1-C4	38.32 (25)	C4-C5-C6	119.44 (62)	F3-P1-F1	90.87 (39)
C3-Fe1-C9	100.96 (31)	C8-Fe1-C5	79.67 (27)	C7-C6-C5	105.02 (63)	F3-P1-F2	90.93 (32)
C3-Fe1-C8	85.84 (33)	C8-Fe1-C7	37.24 (30)	C8-C7-C6	119.45 (73)	F3-P1-F4	88.44 (33)
C3-Fe1-C5	165.36 (31)	C8-Fe1-C4	68.50 (29)	C7-C8-C9	121.09 (70)	F1-P1-F2	90.38 (30)
C3-Fe1-C7	100.95 (33)	C5-Fe1-C7	66.01 (29)	C4-C9-C8	118.34 (65)	F1-P1-F4	89.13 (30)
C3-Fe1-C4	136.84 (30)	C5-Fe1-C4	37.66 (24)	F5-P1-F6	92.32 (43)	F2-P1-F4	179.20 (51)
C2-Fe1-C9	155.02 (32)	C7-Fe1-C4	79.50 (28)	F5-P1-F3	88.86 (40)		

b. B

Bond Distances

Fe1-C1	1.795 (10)	Fe1-C7	2.245 (8)	C4-C9	1.422 (10)	C8-C9	1.402 (12)
Fe1-C3	1.814 (9)	C1-O1	1.147 (11)	O4-C10	1.433 (10)	P1-F4	1.505 (8)
Fe1-C2	1.899 (12)	C2-O2	1.059 (13)	C5-C6	1.513 (11)	P1-F1	1.517 (8)
Fe1-C9	2.077 (8)	C3-O3	1.118 (10)	C6-C7	1.518 (12)	P1-F3	1.540 (10)
Fe1-C8	2.122 (7)	C4-O4	1.349 (10)	C7-C8	1.382 (12)	P1-F5	1.571 (7)
Fe1-C5	2.165 (7)	C4-C5	1.379 (11)	C7-C11	1.503 (14)	P1-F2	1.578 (5)
Fe1-C4	2.172 (7)						

Bond Angles

C1-Fe1-C3	92.04 (45)	C2-Fe1-C9	152.94 (33)	C5-Fe1-C7	65.98 (30)	C11-C7-C6	118.22 (80)
C1-Fe1-C2	97.37 (40)	C2-Fe1-C8	123.12 (35)	C4-Fe1-C7	79.25 (31)	C7-C8-C9	122.33 (68)
C1-Fe1-C9	101.93 (40)	C2-Fe1-C5	89.76 (34)	O1-C1-Fe1	179.30 (99)	C8-C9-C4	118.34 (77)
C1-Fe1-C8	139.29 (40)	C2-Fe1-C4	125.83 (34)	O2-C2-Fe1	177.05 (82)	F4-P1-F1	95.23 (81)
C1-Fe1-C5	98.34 (39)	C2-Fe1-C7	87.93 (33)	O3-C3-Fe1	178.77 (93)	F4-P1-F3	177.05 (87)
C1-Fe1-C4	85.05 (36)	C9-Fe1-C8	38.98 (33)	O4-C4-C5	125.67 (62)	F4-P1-F5	90.32 (64)
C1-Fe1-C7	163.54 (39)	C9-Fe1-C5	68.91 (29)	O4-C4-C9	115.57 (76)	F4-P1-F2	90.72 (51)
C3-Fe1-C2	97.31 (41)	C9-Fe1-C4	39.02 (29)	C5-C4-C9	118.04 (78)	F1-P1-F3	87.60 (77)
C3-Fe1-C9	100.75 (38)	C9-Fe1-C7	68.57 (33)	C4-O4-C10	118.56 (68)	F1-P1-F5	174.11 (71)
C3-Fe1-C8	87.16 (39)	C8-Fe1-C5	79.45 (31)	C4-C5-C6	118.85 (66)	F1-P1-F2	89.82 (39)
C3-Fe1-C5	166.61 (35)	C8-Fe1-C4	68.74 (31)	C5-C6-C7	104.82 (67)	F3-P1-F5	86.81 (76)
C3-Fe1-C4	136.81 (37)	C8-Fe1-C7	36.75 (32)	C8-C7-C11	122.04 (77)	F3-P1-F2	90.10 (45)
C3-Fe1-C7	102.77 (38)	C5-Fe1-C4	37.07 (29)	C8-C7-C6	117.33 (80)	F5-P1-F2	92.05 (36)

structure factor amplitudes. In the least-squares refinement, the agreement indices $R_1 = \sum(|F_o| - |F_c|)/\sum|F_o|$ and $R_2 = (\sum w(|F_o| - |F_c|)^2/\sum w|F_o|^2)^{1/2}$ were used. The atomic scattering factors are from ref 11.

Least-squares refinement results using anisotropic thermal parameters for all non-hydrogen atoms are shown in Table I. Positions for all hydrogen atoms connected to carbon atoms were calculated and added as fixed contributors by using a bond distance of 0.95 Å and an isotropic temperature factor equal to 1.1 times the temperature factor of the atom the hydrogen is bonded to.

Parts a and b of Figure 1 show the structures of A and B, respectively. Final positional parameters with estimated standard deviations are shown in parts a and b of Table II, respectively. Parts a and b of Table III list the crystallographically determined bond distances and angles. Anisotropic thermal parameters with their estimated standard deviations and listings of observed and calculated structure factor amplitudes are available as supplementary material.

The general features of compounds A and B are similar to those of other cyclohexadienyl complexes reported in the literature.[12] One CO of $Fe(CO)_3$ eclipses the methylene group. The five carbon atoms forming the dienyl part, C_4, C_5, C_9, C_8, C_7, are practically coplanar. C_6 is situated above the dienyl plane on the opposite side of the metal (perpendicular distance C_6 to the dienyl plane is 0.549 Å in A and 0.576 Å in B). The angles between the planes 4–5–9–8–7 and 5–6–7 are 37.5° in A and 39.1° in B. Similar values ranging from 39° to 43° have been obtained in other cyclohexadienyl complexes. The bonding distances of the iron center to the dienyl carbon atoms are of special interest for us. They vary from 2.111 to 2.190 Å in A and from 2.077 to 2.245 Å in B. An earlier report of A[12a] gives significantly larger Fe–C distances, but a full discussion of this earlier structure is not available.

The mirror plane bisecting the cyclohexadienyl is only an approximation here due to the unsymmetrical substitution. Significant differences exist. In A, FeC_5 (2.172 (6) Å) is slightly shorter than FeC_7 (2.186 (8) Å) while FeC_4 (2.190 (7) Å) is longer

(11) "International Tables for X-ray Crystallography"; Ibers, J. A., Hamilton, W. C., Eds.; Kynoch Press: Birmingham, England, 1974: Vol. IV, Table 2.2 and Table 2.3.1.

(12) (a) Mason, R. 23rd IUPAC Congress, Boston, 1971, Vol. 6, p.31. (b) Semmelback, M. F.; Hall, H. T., Jr.; Farina, R.; Yoshifuji, M.; Clark, G.; Bargar, T.; Hirotsu, K.; Clardy, J. *J. Am. Chem. Soc.* **1979**, *101*, 3535. Bailey, N. A.; Blunt, E. H.; Fairhurst, G.; White, C. *J. Chem. Soc., Dalton Trans.* **1980**, 829. Bottrill, M.; Green, M.; O'Brien, E.; Smart, L. E.; Woodward, P. *Ibid.* **1980**, 292. Etermadi, B.; Moss, D. S.; Palmer, R. A. *J. Inorg. Nucl. Chem.* **1981**, *43*, 1997. (c) Janse Van Nuuren, P.; Fletterich, R. J.; Meinwald, J.; Hughes, R. E. *J. Am. Chem. Soc.* **1971**, *93*, 4394.

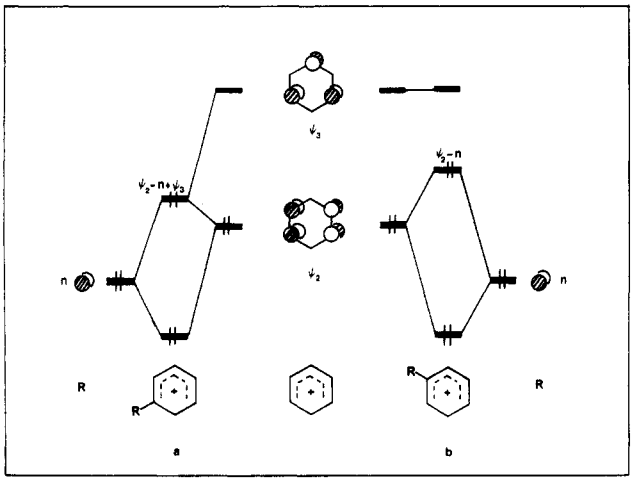

Figure 2. Interaction diagram between a $Fe(CO)_3$ fragment and a cyclohexadienyl cation ligand.

than FeC_8 (2.124 (7) Å). In B, FeC_5 (2.165 (7) Å) is considerably shorter than FeC_7 (2.245 (8) Å) while FeC_4 and FeC_8 are more equal (2.172 (7) vs. 2.122 (7) Å). Clearly, the Fe center is not equally bonded to the two ends of the dienyl. An analogous distortion of the bonding has been observed in another unsymmetrically substituted cyclohexadienyl.[12c] As in our compound B, the more pronounced effect was unequal metal to terminal carbon distances. We will see below that this above distortion has an important effect on the reactivity of the complex.

Theoretical Analysis of the Formation and Reactivity of the Cyclohexadienyl Complex

A. Hydride Abstraction. A theoretical analysis of the regioselectivity of hydride abstraction is always a difficult problem. First, the charge taken by a hydrogen atom in a CH bond is usually small and rather insensitive to the nature of the atoms linked to the carbon. Second, the molecular orbitals characteristic of a CH bond are spread over the whole spectrum of the MOs of the molecule. Therefore, a perturbational analysis involving a CH bond is especially difficult to make. In our case, it is likely that the transition state for hydride abstraction is productlike and consequently the position of hydride abstraction reflects the strength of metal dienyl bonding in the resultant dienyl complexes.

The bonding and conformational properties of tricarbonyliron cyclohexadienyl cation complex have been previously analyzed.[13] A summary of the results is shown in Figure 2. The $Fe(CO)_3$ fragment has two degenerated hybrides of e symmetry which we call $2e_s$ (symmetric with respect to the symmetry plane of the whole complex) and $2e_a$ (antisymmetric with respect to the same plane) and a $2a_1$ hybrid higher in energy. It also has three lower d orbitals that are acting mostly as lone pairs and are weakly involved in bonding with the ligands ($1a_1$, $1e_s$, $1e_a$). For a neutral $Fe(CO)_3$ fragment, two electrons go into the 2e hybrids and six into the low-lying d block. The cyclohexadienyl cation ligand has five π orbitals, two of which are occupied. In Figure 2, we have schematically represented the π orbitals of the cyclohexadienyl as those of a dienyl. For our purpose, it is sufficient. The exact electronic structure of a cyclohexadienyl complex has been discussed by Hoffmann and Hofmann.[13] The lower occupied orbital ψ_1 does not give rise to a large metal–ligand interaction because it is far away from the $2a_1$ metal hybrid. The HOMO ψ_2 that is antisymmetric with respect to the mirror plane finds a match with $2e_a$. It is perturbed by $1e_a$ and spread between two levels 1a″ and 2a″. The LUMO ψ_3 overlaps with $2e_s$ to give the bonding 3a′ and antibonding 4a′ orbitals. Higher in energy one finds ψ_4, which has the same symmetry as ψ_2, and does act as a perturbation and also appears in the vacant MOs that will be discussed later on. ψ_5 is too high in energy and has too many nodes to add anything to the bonding scheme.

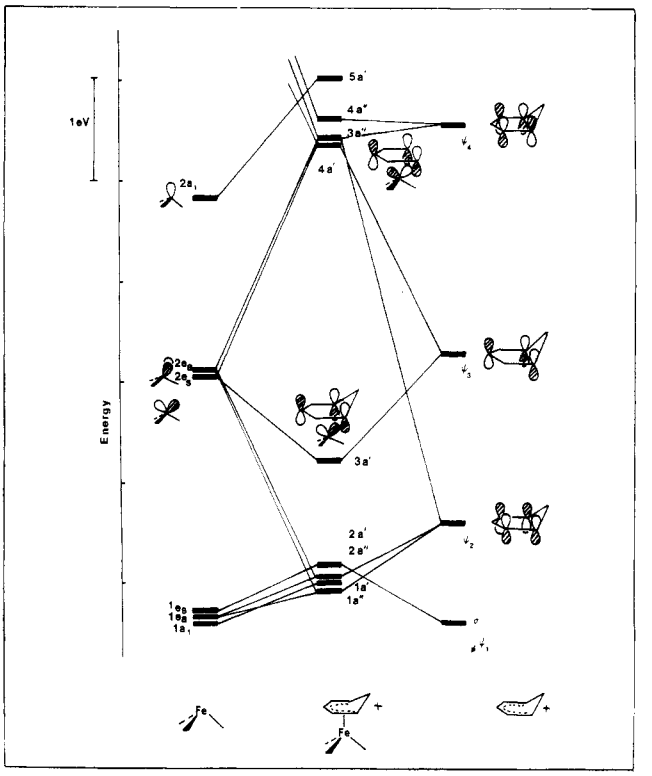

Figure 3. Interaction diagram between a π electron donor, R, and cyclohexadienyl frontier orbitals.

Most of the analysis can be limited to the interaction of the metal 2e set with the dienyl ψ_2 and ψ_3 because of their proximity in energy. The four electrons of the frontier orbitals go into bonding orbitals $\psi_2 + 2e_a$ and $\psi_3 + 2e_s$. It is clear that it is favorable for the system to bring the frontier MOs of the cyclohexadienyl close to the metal 2e set. One therefore needs to raise the HOMO and/or lower the LUMO of the dienyl ligand. Such tuning is achieved by adequate substitution.

Due to the nodal properties of the HOMO ψ_2, **11**, and the LUMO ψ_3, **12**, substituents have no effect on the

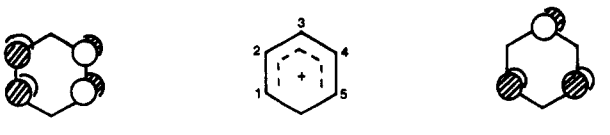

ψ_2 ψ_3

11 **12**

HOMO if placed at C_3 and no effect on the LUMO if placed at C_2 and C_4. π donor groups raise the energy of the HOMO if placed at C_1 and C_2. The destabilizing effect created by a π donor group is less at C_1 than at C_2. If a substituent is put at C_1, ψ_3 stabilizes the antibonding combination of ψ_2 and the substituent lone pair (Figure 3a), an effect which is not desired. A substitution at C_2 prevents ψ_3 that has a node at this position to come into play (Figure 3b).

(13) Hoffmann, R.; Hofmann, P. *J. Am. Chem. Soc.* **1976**, *98*, 107. For a bonding analysis in (cyclohexadienyl)PtL_2 see: Mingos, D. M. P.; Nurse, C. R. *J. Organomet. Chem.* **1980**, *184*, 281.

Table IV. Energy Levels of the Frontier Orbitals of Substituted Cyclohexadienyl Cations

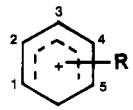

R	substd atom	HOMO, eV	LUMO, eV
OCH_3	C_1	−12.291	−10.476
	C_2	−12.195	−10.759
	C_3	−12.409	−10.463
CO_2CH_3	C_1	−12.419	−11.047
	C_2	−12.452	−10.766
	C_3	−12.436	−11.066

A similar argument applies to π acceptor groups. They stabilize ψ_3 if placed at C_1 and C_3. The stabilization of ψ_3 is smaller for a substitution at C_1 because the HOMO ψ_2 mixes into ψ_3 in an antibonding way. This second-order mixing does not occur when the substituent is at C_3.

Extended Hückel calculations of 1-, 2-, and 3-methoxy- and 1-, 2-, and 3-carbomethoxycyclohexadienyl cations confirm the qualitative trend (Table IV). The 2-methoxycyclohexadienyl has the highest HOMO and also the lowest LUMO. The 3-carbomethoxycyclohexadienyl has the lowest LUMO. Note that the difference between C_1 and C_3 substitution is small.

The comparison of the above theoretical results with the experimental facts is rewarding. Only the 2-methoxy- and the 3-carbomethoxycyclohexadienyl complexes are observed from the hydride abstraction of the 2-substituted diene complex. In **6**, the hydride abstraction puts the best π donor OMe at the C_2 position.

Note that the preferred substitution pattern on a tricarbonylcyclohexadienyliron complex is different from the one occurring in an isolated cyclohexadienyl cation. For instance, the protonation of anisole occurs preferentially at the para carbon center to give the 3-methoxycyclohexadienyl cation **13**.[14] Our analysis gives also the correct

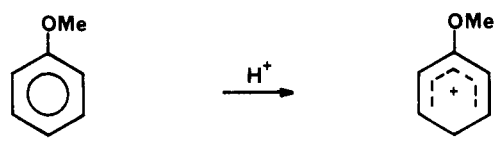

13

substitution pattern. In order to get the most stable cation, one should want to have the LUMO of the dienyl part ψ_3 stabilizing the oxygen lone pair. Thus one selects the ortho and para carbons. A destablizing influence of ψ_2 occurs for a substitution at the ortho carbon not at the para one, which becomes the best position.

The regioselectivity of the Birch reduction has been rationalized with a similar argument on cyclohexadienyl radical and cyclohexadienyl anion.[15]

B. Nucleophilic Addition to the Cyclohexadienyl Cation Complex. A theoretical analysis, based on INDO calculations, of the regioselectivity of the nucleophilic addition to the tricarbonylcyclohexadienyliron complex has been reported.[16] The authors found that the total charge and the π electron density at each carbon do not correlate with the experimental preferred site of attack but that the magnitude of the free valence index, which represents the extent to which an atom is bonded to the other ones, correlates with the experimental facts. The terminal carbon atoms have the smallest free valence index. They are therefore more likely to create a new bond with an incoming reagent.

Table V. π and Total Charges in Cyclohexadienyl Cations and Cyclohexadienyl Cation Complexes[a]

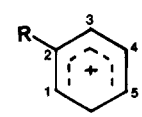

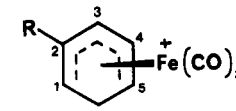

R		q_π	q_{TOT}	q_π	q_{TOT}
H	C_1	0.309 (0.325)	0.255 (0.038)	−0.030	−0.075
	C_2	−0.015 (−0.069)	−0.044 (−0.218)	0.151	0.133
	C_3	0.285 (0.383)	0.258 (0.070)	0.036	0.016
	C_4	−0.015 (−0.069)	−0.044 (−0.218)	0.151	0.133
	C_5	0.309 (0.325)	0.255 (0.038)	−0.030	−0.075
OMe	C_1	0.218	0.131	−0.073	−0.148
	C_2	0.065	0.488	0.200	0.629
	C_3	0.350	0.215	0.007	−0.024
	C_4	−0.009	−0.036	0.150	0.134
	C_5	0.288	0.229	0.033	−0.080

[a] Values in parentheses are coming from ab initio calculations.[17]

Our approach is somewhat different although it will be shown that a weak FeC bond indicates a probable center of reactivity of the carbon in question.

Let us first discuss briefly the charges at the cyclohexadienyl cation. The π and total charges for an isolated cyclohexadienyl cation, a $Fe(CO)_3$ cyclohexadienyl cation complex, and their corresponding 2-methoxy derivatives are given in Table V. In the isolated cation the charges alternate as expected in this type of molecule. The ortho and para carbons are positively charged; the meta is negatively so. Charges are quite large, a characteristic of EHT calculations. Values derived from an ab initio calculation (in parentheses) are given for comparison.[17] π charges are similar in both calculations, but the total charges differ in magnitude. Positive charges are small and negative charges large in the ab initio results.

The coordination to the $Fe(CO)_3$ fragment dramatically modifies the charges at the different centers. Charge alternation disappears; C_1 is π negatively charged; C_2 and C_3 are π positively charged. Total charges are similar. These modifications in the charge distribution upon complexation to the metal are due to the familiar donation/back-donation effect. The cyclohexadienyl is donating electrons through its HOMO ψ_2. It is therefore losing electrons at C_1 and C_2 but not at C_3. On the other hand, the LUMO ψ_3 receives some electrons that accumulate at C_1 and C_3. Although the quantity of charge transfer cannot be predicted, one understands why C_2 has become more positive and C_1 and C_3 less so. Despite the difficulty in describing charges with EHT calculations, we believe that the variation of the charges between the noncoordinated and coordinated ligands is qualitatively correct.

The methoxy group perturbs the above charge distribution. All carbon centers but C_2 and C_4 are negatively charged. It is therefore apparent that charge control of the nucleophilic addition does not explain the observed regioselectivity because the nucleophile prefers to add to a relatively negatively charged center (C_5 or C_1).

(14) Olah, G. A.; Mo, Y. K. *J. Org. Chem.* **1973**, *38*, 353.
(15) Birch, A. J.; Hinde, A. L.; Radom, L. *J. Am. Chem. Soc.* **1980**, *102*, 3370, 4074, 6430.
(16) Clark, D. W.; Monski, M.; Kane-Maguire, L. A. P. *J. Organomet. Chem.* **1976**, *107*, C40. Similar calculations have been done on the chromium complex: *Ibid.* **1976**, *120*, C25.
(17) Binning, R. C., Jr.; Sando, K. M. *J. Am. Chem. Soc.* **1980**, *102*, 2948. Hehre, W. J.; Pople, J. A. *Ibid.* **1972**, *94*, 6901.

Table VI. Iron-Carbon Bond Orders for Substituted Cyclohexadienyliron Complexes

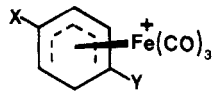

	X = H, Y = H	X = OMe, Y = H	X = OMe, Y = Me
FeC_1	0.220	0.229	0.227
FeC_2	0.043	0.084	0.092
FeC_3	0.134	0.133	0.133
FeC_4	0.043	0.091	0.093
FeC_5	0.220	0.221	0.216

Let us now discuss the lowest set of vacant molecular orbitals of the complex, which we know must play an important role in controlling the addition of a nucleophile.

A group of three molecular orbitals appears at a low energy (Figure 2). The lowest one 4a′ is made of the antibonding combination of ψ_3 and $2e_s$. The antibonding combination of $2e_a$ and ψ_2 stabilized by the empty dienyl ψ_4 makes 3a″, which is almost degenerate in energy with 4a′. Finally, above 4a′ and 3a″ one finds 4a″ that is made of ψ_4 mixing in an antibonding fashion with $2e_a$ and stabilized by some higher metal fragment orbitals. 4a′ has large coefficients on C_1, C_3, and C_5 while 3a″ has small coefficients on C_1 and C_5. The reason for these small coefficients is depicted in 14. ψ_4 mixes with $2e_a$ mostly

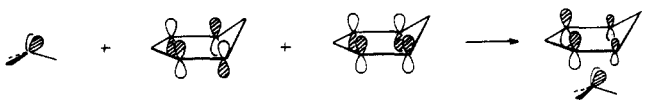

14

via the terminal carbons C_1 and C_5. This is due to the fact that $2e_a$ is tilted away from the two CO groups that are not in the mirror plane. Therefore, the in-phase mixing of ψ_4 into $2e_a$ diminishes the lobes at C_1 and C_5. 4a″ has large coefficients on C_1, C_2, C_4, and C_5.

The relative energy of the lowest MOs depends on the nature of the ligands on the metal. Replacement of the CO groups by model H^- leads to 3a″ being more stable than 4a′, although their energies remain close. 4a″ remains higher in energy.

As stated earlier, a nucleophilic addition for these particular complexes occurs preferentially at the terminal carbon. The above analysis suggests a reason for this behavior. The terminal carbons C_1 and C_5 contribute to the three vacant MOs while, due to the nodal properties of these orbitals, C_2, C_3, and C_4 do not contribute to some of them. In terms of orbital control, there is a larger change for the nucleophile to add at the terminal centers. A more quantitative analysis of the reaction is not feasible presently due to the complicated reaction path involved here and the well-known deficiency of the EHT method in describing bond formation and bond cleavage.

Let us analyze now the consequences of the introduction of a π donor group in an unsymmetrical fashion on the cyclohexadienyl. We first discuss the structural changes occurring in the complex and then relate those structural changes to the reactivity toward a nucleophile. We focus our attention on substitution at C_2.

The π donor group at C_2 distorts the π orbitals of the cyclohexadienyl so that the carbons on each side of the former mirror plane do bond unequally to the metal center. The metal–carbon overlap populations in the reference substituted cyclohexadienyl complex and in the 2-methoxy-substituted complex illustrate these points (Table VI). From the value of the metal–carbon overlap population in the parent complex, it is clear that C_1, C_3, and C_5 are more strongly attached to the metal than C_2 and C_4. The iron center is therefore in a pseudooctahedral field. The directionality of the 2e hybrid orbitals of $Fe(CO)_3$ indicates the reasons for this bonding pattern. $2e_s$ overlaps with C_1, C_3, and C_5, and $2e_a$ is tilted in such a way as to overlap more with C_1 and C_5 than with C_2 and C_4 (Figure 1).

In the 2-methoxy- and 2-methoxy-5-methylcyclohexadienyl complex[18] the FeC_1 overlap population is larger than that of FeC_5 (0.229 and 0.227, respectively, vs. 0.221 and 0.216, Table VI). Consequently, the FeC_1 bond should be shorter than the FeC_5 one. This is indeed observed in the two structures A and B. The difference is small in the 2-methoxy-substituted one (FeC_5 = 2.172 Å, FeC_7 = 2.186 Å, Figure 1a) and may not be crystallographically significant. In contrast, it is much larger in the disubstituted complex (FeC_5 = 2.165 Å, FeC_7 = 2.245 Å, Figure 1b) and crystallographically significant. Therefore in both systems the metal fragment is moved toward the side of the dienyl containing the π donor group. The larger distortion in structure B does not correlate with the values of the FeC_1–FeC_5 overlap population because the difference between these two values is the same in the 2-methoxy and 2-methoxy-5-methyl complex. Some steric hindrance between the methyl group and the $Fe(CO)_3$ moiety may be responsible for the additional distortion. A similar distortion of the metal fragment upon substitution has been noticed.[12c] In 15, the FeC_1 and FeC_5 distances are, respectively, 2.149 and 2.291 Å. Some strain may be responsible for such a large difference although the authors do not find unusual structural features in the side chain that links the iron to C_2.

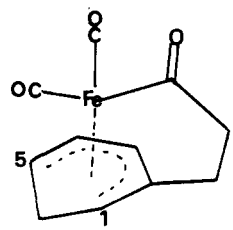

15

The difference in the metal–carbon overlap population is easily related to the shape of the substituted dienyl HOMO. The HOMO of the 2-methoxycyclohexadienyl cation as shown in 16 has larger coefficients at C_1 and C_2

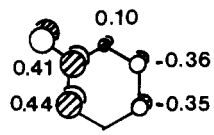

16

than at C_4 and C_5. This dissymmetry originates from a mixing out-of-phase of the lower ψ_1 π orbital into ψ_2 that is produced by their common antibonding interaction with the oxygen lone pair, 17. In contrast, the LUMO ψ_3 is practically not perturbed by the substituent because of the nodal plane at C_2. Consequently, the metal $2e_a$ overlaps better with the dienyl HOMO if it is shifted toward the C_1C_2 side.

Olefin complexes are also distorted when the olefin carries π donor and π acceptor group.[19] Interestingly,

(18) We use this numbering in place of the 1-methyl-4-methoxycyclohexadienyl in order to compare more conveniently with the 2-methoxycyclohexadienyl complex.

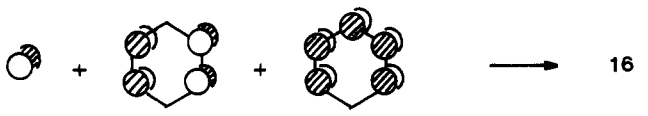

17

while in the olefin complexes the metal is shifted away from the substituted carbon, the opposite distortion is observed in the cyclohexadienyl complex. The examination of the π orbital of the substituted dienyl provides an explanation for this fact.

Unequal bond lengths in a π complex has consequences on its reactivity. It has already been found that a similar distortion is responsible for the regioselectivity of nucleophilic addition to olefin complexes.[20] A similar effect is at work here.[21] To illustrate this point we have performed a calculation of a simplified distortion of the molecule in which the $Fe(CO)_3$ moiety is shifted 0.1 Å perpendicularly from the mirror plane of the cyclohexadienyl. The orbital analysis is shown for the nonsubstituted complex for sake of simplicity. We can consider only the vacant orbital derived from 4a′ because it has the largest coefficients at the terminal carbons. The orbital is strongly perturbed by the displacement of the metal. The coefficients on the dienyl fragment shown in **18** illustrate the localization of the orbital on the carbon

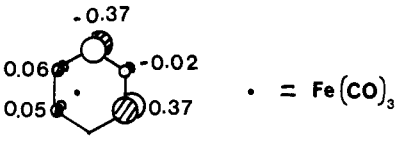

18

C_5 that is further away from the metal. The shape of **18** comes from a complicated mixing of the π orbitals of the ligand under the influence of the metal. The major contribution to **18** is the LUMO of the dienyl ψ_3 and the two orbitals ψ_4 and ψ_2 next to them in energy. They mix as shown in **19**. There is no doubt that this distortion strongly activates C_5 with respect to C_1 toward the nucleophile.

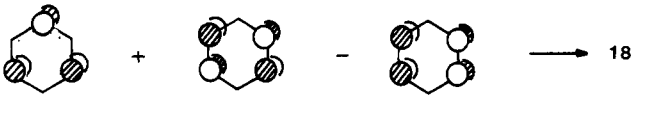

19

The results of this study can be summarized in the following manner. The hydride abstraction from the tricarbonyliron diene complex produces the apparently most stable dienyl complex. The regioselectivity of the nucleophilic addition to the cyclohexadienyl complex comes from a subtle substituent effect. The π donor substituent causes a slipping of the metal that partially decoordinates the terminal carbon further away from the substituent. This terminal carbon becomes therefore very reactive toward a nucleophile.

It is therefore apparent that small distortions within a molecule may have large consequences on the reactivity. Conformational effects were found to be responsible for the reactivity of (arene)chromium tricarbonyl complexes.[22] Unequal metal–carbon bond lengths are important factors in the reactivity of coordinated olefin and cyclohexadienyl complexes.

Acknowledgment. O.E. acknowledges the donors of the Petroleum Research Fund, administered by the American Chemical Society, for financial support. A.J.P. is grateful to the National Institutes of Health (GM 30373 and GM 30757) for financial support of research programs. We wish to express our gratitude to Professor Roald Hoffmann for helpful discussions.

Appendix

All calculations were perfomed by using the extended Hückel method with the weighted H_{ij} approximation.[23] The values of H_{ii} are those of ref 13. C–C(dienyl) = 1.4 Å. Standard bond lengths were taken for the other bonds in the cyclohexadienyl fragment. The CH_2 group is bent by 40° with respect to the dienyl plane. Fe–(center of dienyl) = 1.82 Å; C–O ($Fe(CO)_3$) = 1.15 Å, angle (OC)–Fe–(center of dienyl) = 135°.

Registry No. **2**, 49654-90-2; **4** (R = OCH_3)·PF_6, 51508-59-9; **4** (R = OCH_3), 46357-52-2; **7**·PF_6, 79777-08-5; 1-methoxycyclohexadienyl cation, 90134-34-2; 2-methoxycyclohexadienyl cation, 81643-53-0; 3-methoxycyclohexadienyl cation, 37396-37-5; 1-methoxycarbonylcyclohexadienyl cation, 90134-35-3; 2-methoxycarbonylcyclohexadienyl cation, 90134-36-4; 3-methoxycarbonylcyclohexadienyl cation, 90134-37-5; cyclohexadienyl cation, 26812-57-7.

Supplementary Material Available: Tables of anisotropic temperature factors and observed and calculated structure factor amplitudes for A and B (20 pages). Ordering information is given on any current masthead page.

(19) Albright, T. A.; Hoffmann, R.; Thibeault, J. C.; Thorn, D. L. *J. Am. Chem. Soc.* **1979**, *101*, 3801.

(20) (a) Eisenstein, O.; Hoffmann, R. *J. Am. Chem. Soc.* **1981**, *103*, 4308. Fujimoto, H.; Koga, N. *Tetrahedron Lett.* **1982**, 4357. (b) Chang, T. C. T.; Foxman, B. M.; Rosenblum, M.; Stockman, C. *J. Am. Chem. Soc.* **1981**, *103*, 7361. Wright, L. L.; Wing, R. R.; Rettig, M. F. *Ibid.* **1982**, *104*, 610. Goel, A. B.; Goel, S.; van der Veer, D. *Inorg. Chim. Acta* **1982**, *65*, L205. Maresca, L.; Natile, G. *J. Chem. Soc., Chem. Commun.* **1983**, 40. (c) A similar distortion has been suggested in the addition to allyl complexes: Keinan, E.; Roth, Z. *J. Org. Chem.* **1983**, *48*, 1769. (d) The fluxional behavior of cyclohexadienyl complexes of platinum was discussed: Mingos, D. M. P.; Nurse, C. R., ref 13.

(21) A related suggestion has been made: Birch, A. J.; Stephenson, G. R. *J. Organomet. Chem.* **1981**, *218*, 91.

(22) Albright, T. A.; Carpenter, B. K. *Inorg. Chem.* **1980**, *19*, 3092.

(23) Ammeter, J. H.; Bürgi, H.-B; Thibeault, J. C.; Hoffmann, R. *J. Am. Chem. Soc.* **1978**, *100*, 3686.